39 Ignition Characteristics of Flanged Electrode in Premixed Gaseous Flow Field

Kenichi OKAMOTO[1], Keita ENDOH[1]
Hiroshi YAMASAKI[2], Hiroshi NOMURA[2], Yasushige UJIIE[2], Kazuhiro ISHII[3]
[1] Graduate School of Industrial Technology, Nihon University,
[2] Nihon University, [3] Yokohama National University

1-2-1 Izumi-cho, Narashino, Chiba 275-8575, Japan

Experimental and numerical studies have been carried out to obtain the detail information about the ignition characteristics of the flanged electrodes in the premixed gaseous flow field. The propane-air premixed swirling flow field was prepared in the cylindrical constant-volume chamber. The flow field was measured by using LDV for various swirling rates prior to the ignition experiments. The result shows that the stable velocity reduction has been caused around the electrodes mounting the flanges. It is concluded that the effect of flanges on the flow field affects on the reduction of minimum ignition energy. The supplied heat dissipation of flow field around the flanged electrodes have been evaluated numerically.

***Keywords*: Engine, Engine Combustion, Lean-burn, Swirling Flow, Flanged Electrode, Numerical Analysis**

1. INTRODUCTION

Reducing harmful emissions and increasing fuel efficiency in the internal combustion engines are urgent problems. Lean-burn technology would be regarded as promising one of the solutions to improve the present matters. In the lean-burn environment, turbulence generated by the swirl or the tumble is utilizing to promote the flame propagation. However, the higher turbulent intensity in the combustion field causes a decrease of ignition probability and it results in frequent occurrences of misfire in the actual engine operations. They are caused by an increase of the heat release from the flame kernel with an increase of turbulent intensity around the ignition electrode. One to improve the igniter probability is sufficient supply of ignition current for ignition. However, an excessive ignition current damages the ignition equipment and causes the electromagnetic interference noise. From these reasons, the development of the ignition system achieving the low ignition energy with a high ignition probability is an important subject for the lean-burn method and the spark-ignition engine.

A number of studies have been carried out the ignition of gas burning environment or similar one. They are classified into two groups from the point of view of concepts and experimental methods. One is a chemical approach[(1)-(2)] in which the ignition process and characteristics are investigated from the chemical or microscopic point of view. The other is the investigation on the ignition aspects affected of the physical conditions[(3)-(4)], in which are studied to explore the physical effects like the flow field. A review of the literature indicates that the ignition processes of lean-burn environment have not yet been clarified sufficiently to utilization of lean-burn in any actual combustors or engines.

Experimental study have been carried out to clarify the effect of flange mounting to the electrode for improving the ignition characteristics in natural gas environment[(5)]. The experimental results in constant-volume combustion chamber study indicated that the minimum ignition energy decreases by flanged electrode in lean burn quiescent environment. It was also observed that the shock wave refraction with the flanges prevents the energy dissipation of the spark discharge. Primary objective of present work is to obtain the detail information about the ignition characteristics of the flanged electrode in the premixed gaseous flow field. The stable propane-air premixed swirling flow field was generated in the cylindrical constant-volume chamber for the various swirling rate. The ignition experiment was carried out using the flanged or normal electrode. The flow field was measured using a Laser Doppler Velocimetry (LDV) with ignition simultaneously. The effects on flow field of the flange mounting were revealed experimentally. Three-dimensional numerical analysis has been done to support the experimental results. Effects on supplied heat dissipation of flow field around the flanged electrode have been evaluated.

2. EXPERIMENTAL APPARATUS AND PROCEDURE

Figure 1 shows the schematics of the combustion chamber. The combustion chamber is made of stainless steel (SUS303), with the inner diameter of 60 mm and width of 25 mm. Two windows made by quarts glass is with the thickness of 15 mm were installed in the sidewall for observation and LDV measurements. The electrode tested was mounted vertically at the top of the combustion chamber. A blow nozzle with the diameter of 2 mm is installed along the sidewall of combustion chamber for tangential blow charging. The configuration of flanged electrode used in the present study is shown in Fig. 2. The cylindrical insulator for supporting the flanged electrodes with the diameter of 10 mm was used. The flanges were made of brass disc with the diameter of 9 mm and the thickness of 1.6 mm. The flange distance and the gap of electrode were keeping at 4smm and 1smm respectively. The center of electrode was set at the r_e=20 mm of radial distance and θ_e =90 degrees of tangent angle in of the cylindrical coordinate, where the origin of θ_e is defined as the horizontal axis just after the blow nozzle.

Figure 3 shows the schematics of the experimental apparatus for ignition measurement. It consists of the swirling flow generator, the ignition system, and its measurement devices. The swirling flow generator consists of an air compressor, a vacuum pump, a fuel-air mixture tank, a solenoid valve, an air regulator, a propane cylinder, a flow control valve. The combustion chamber pre-evacuated by a vacuum pump is filled with propane-air mixture feed from the mixture tank. After the time for forming the quiescent gas field, a premix gas was blow in to generate the swirling flow using an air cylinder and solenoid valves. The ignition system consists of a transistorized ignition system, a battery (12V), a variable resistor, a pulse generator, and a function generator. A current for spark discharge were varied by resistance of the variable resistor. The primary current for spark ignition was measured by a current probe and an oscilloscope. Minimum ignition energy in this study was defined that the primary current with the ignition achieving in the 50 % of 30 runs.

Measurements of flow field in the combustion chamber, in the region between the flanges and the region flanged have been done prior the ignition experiment. Figure 4 represents the experimental set up of flow

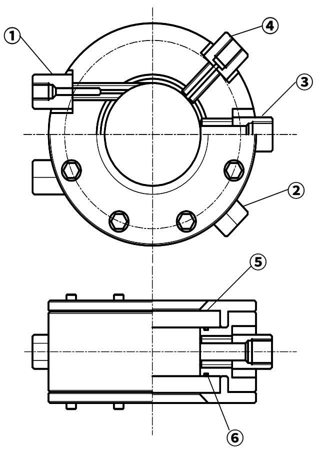

1. Nozzle
2. Exhaust port
3. Electrode holder
4. Particle port
5. Quartz glass
6. O-ring

Fig. 1 Combustion chamber.

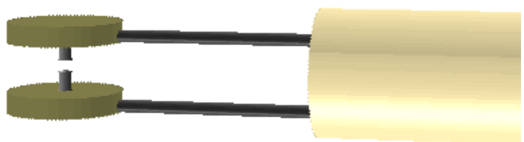

Fig. 2 Configuration of flanged electrode.

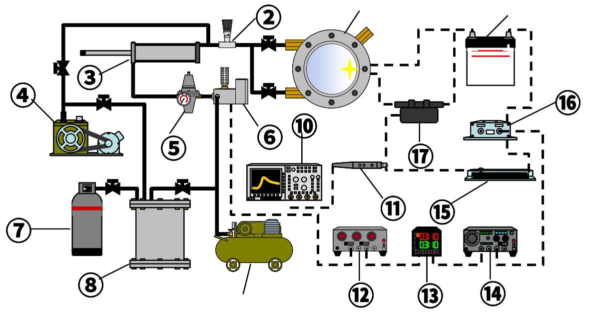

1. Chamber	2. Flow control valve
2. Air cylinder	4. Vacuum pump
5. Air regulator	6. Solenoid valve
7. Propane gas	8. Mixture tank
9. Air compressor	10. Oscilloscope
11. Current probe	12. Pulse generator
13. Delay generator	14. Function generator
15. Variable resistance	16. Igniter
17. Ignition coil	18. Battery

Fig. 3 Schematic diagram of experimental apparatus.

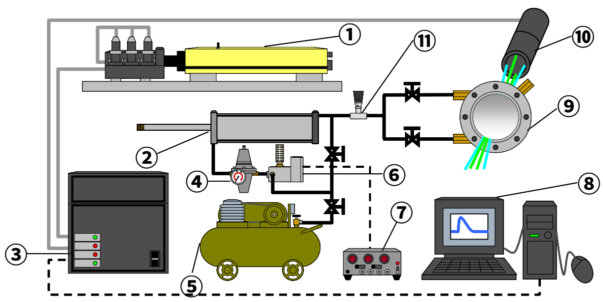

1. Argon-ion laser	2. Air cylinder
3. LDV detector unit	4. Air regulator
5. Air compressor	6. Solenoid valve
7. Pulse generator	8. Personal computer
9. Chamber	10. LDV probe
11. Flow control valve	

Fig. 4 Experimental setup of flow measurements.

measurement. The measurement system consists of LDV (DANTEC Co.Ltd) and an Ar-ion laser, a personal computer, a function generator, a pulse generator and a delay timer. Two dimensional flow velocity and turbulent intensity at the arbitrary position in the chamber were measured simultaneously by using LDV at the arbitrary time delayed after the gas blown in. The weak concentration of smoke was used as the tracer particle. The radial and tangential velocity was measured on the central plane in depth to the combustion chamber. The swirling flow was controlled by the control valve opening ϕ_c. The swirling flow field in the combustion chamber was grasped by the flow velocity at the positions from 5 mm to 25 mm with every 5 mm in radial direction at the vertical (θ_s = 0˚, 180˚) and horizontal axis (θ_s = 90˚, 270˚). The flow fields between the flanges were also measured at ranging of ±6 mm with 3 mm spacing centered at the electrode in radial direction on the symmetric axis of flanged electrodes.

PHOENICS Version 3.6 of the CHAM Co. Ltd. was used for the numerical analysis. The grid for computation was constituted along three-dimensional Cartesian coordinates. The quadratic upwind scheme, the simple k-ε model and the log-law were applied for computation. The number of grid were 80, 30 and 80 along X, Y, and Z directions respectively. The wall boundary was prepared to simulated the cylindrical chamber with the same configurations. The fan function, which gains the momentum in the arbitrary field, is applied to generate the swirling flow in the chamber. The fan function is prepared on the extension of central axis of blow nozzle. The body, its configuration is similar to the flanged electrode tested, was set up in the numerical field. The steady-state computation made to form the swirling flow field at the ignition timing in the experiment.

The ignition experiments were carried out for the propane-air premixed gas swirling flow. The equivalence ratio was assumed to be constant at 0.753. The driving pressure of the air cylinder to blow in was a constant pressure of 0.539 MPa. Figure 4 shows an example of the typical temporal variation of LDV signal at the center of electrode of ϕ_c=2.0 %. The abscissa represents the composed velocity of radial and tangential direction at the center of the electrode in the swirling field, at the positioned to be (20, 90˚). The ordinate represents the time elapsed. The result shows that the LDV signal rises rapidly at about 20 ms lapsing from the blow starting. The velocity decreases gently with the time elapsed. It is observed that peak means velocity of the swirling flow velocity generated by gas blow was about 10 m/s in the presence conditions. The signal amplitude goes largely with an increase of flow velocity. And it decreases gradually with the decrease of the mean velocity. The regulation time, which is defined as the discharge timing of the spark for ignition synchronizing the swirling flow field, was determined as time to peak of mean flow velocity measured. The mean velocity as the means of measured velocity for the time ranging ±50 ms of the regulation time were used to explore the effects of the flow field on the minimum ignition to combustion.

3. Results and Discussion

Figure 5 shows the mean flow velocity u_s at θ_s = 90˚ in the combustion chamber. The abscissa represents the mean velocity composed radial and tangent direction at the regulation time.

$$\bar{u} = \sqrt{\bar{u}_r^2 + \bar{u}_\theta^2} \quad (1)$$

where, $\bar{u}$, u_r and u_θ represent the mean velocity, velocity for r and θ directions respectively. The ordinate represents the radial coordinates r. The figure demonstrates the effect of control valve openings ϕ_c on the mean flow velocity profiles. The results demonstrate that the flow velocities at the center of the camber and its neighboring were quite small. On the other hand, the mean flow velocities increase with an increase of the radial position. From above result and the case of θ_s = 0˚, 180˚, 270˚, it is concluded that the stable swirling flow would be generated in the test chamber at the regulation time for ignition experiment.

Figure 6 shows the radial turbulent intensity profiles at θ_s = 90˚ for various control valve opening ϕ_c. The

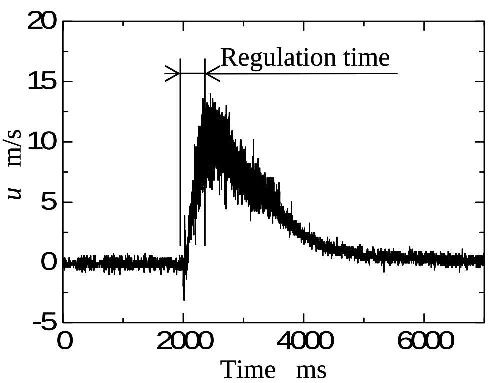

Fig. 4 An example of the typical temporal variation of flow velocity at the center of electrodes in the swirling field (ϕ_c=2.0 %).

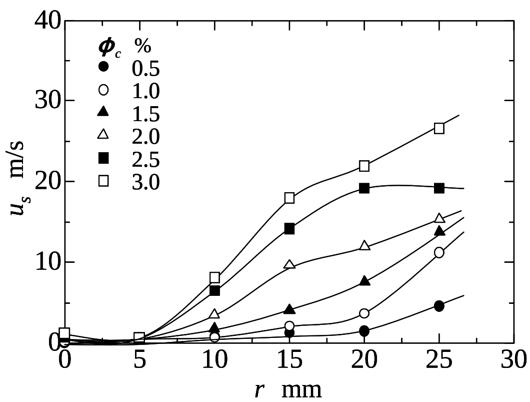

Fig. 5 Radial velocity profiles at θ_s = 90˚ in the combustion chamber.

abscissa represents the time average of the turbulent intensity u_s' given by Eq. (2) at the regulation time.

$$u_s' = \sqrt{\frac{1}{N}\sum_{i=1}^{N}\left(u_i - \overline{u}_s\right)^2} \tag{2}$$

where, u_s', N, u_i, $\overline{u}_s$ are fluctuation of velocity, number of sampling, i component of velocity, mean velocity respectively. It is obvious that the turbulent intensity increases with an increase of radial position. Also it increases with increase of the control valve opening. There is a similar tendency to the its of mean flow velocities. However the turbulent intensity of the central portion was rather large than it at the outer region. The above results suggested that the swirling flow in this study has influenced largely in the flow velocity conditions.

Figure 7 shows the comparison of the measured and numerical results of the velocity profiles of the swirling flow field at θ_s = 90˚. The velocity of control valve opening of 1.0, 2.0 and 3.0 % were shown in Fig. 7. The abscissa and ordinate are the same in Fig. 5. It is clear that the numerical results agree well to the measured results. Also these facts suggest that numerical procedure used in this study is effective for deep understanding of the flow field and has a potential to explore its effect on the ignition phenomena.

Figure 8 show the measured results of the mean flow velocity u_f on the symmetric axis of the flanged electrode. The ordinate represents the radial position on the symmetric axis, which corresponds at θ_s = 90˚. The center of flange and electrode situated at 20 mm. The edges of flanges were located at 15.5 mm and 24.5 mm in radius respectively. It is obvious that the mean flow velocity increases with an increase of ϕ_c. It is also observed that there is not a tendency in the mean flow velocity increasing along the radial direction like the swirling flow field. It is obvious that the mean flow velocities in the flanged region indicate quite lower values than that of swirling field. Figure 9 represents the profiles of turbulent intensity u_f' at the same conditions in Fig. 8. It is obvious that the turbulent intensity have higher values than it in the swirling flow field. Turbulent intensity in the outer region of the flange indicates rather high values at the higher range in ϕ_c. It is conceivable that the occurrences of turbulent generation by an interaction of a flange and swirling flow.

Figure 10 shows the comparison of the mean velocity profiles between the flanged electrode and normal the

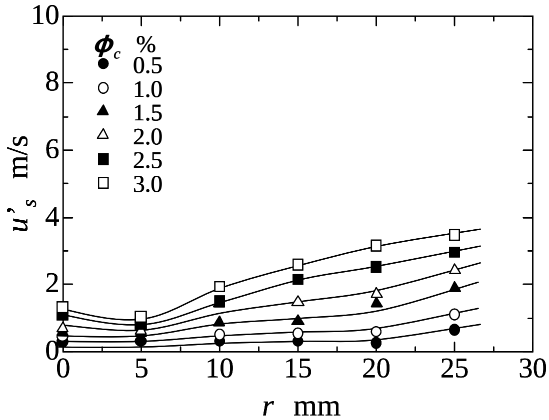

Fig. 6 Radial profiles of turbulent intensity at θ_s = 90˚ in the combustion chamber.

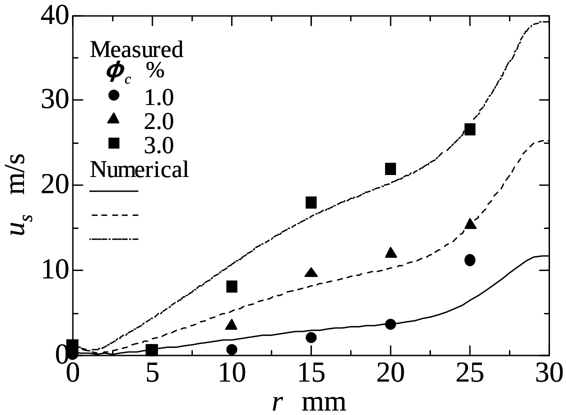

Fig. 7 Comparison between the measured and numerical velocity profiles of swirling flow in the combustion chamber.

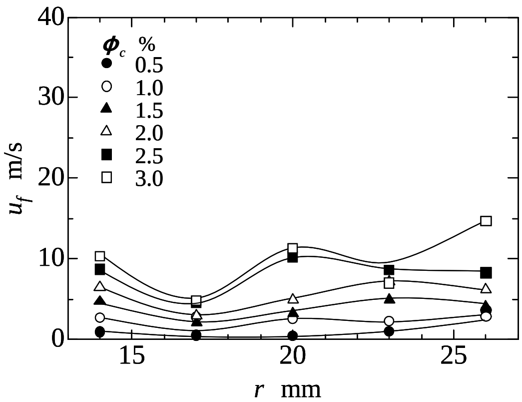

Fig. 8 Mean velocity profiles on symmetric axis of flanged electrode.

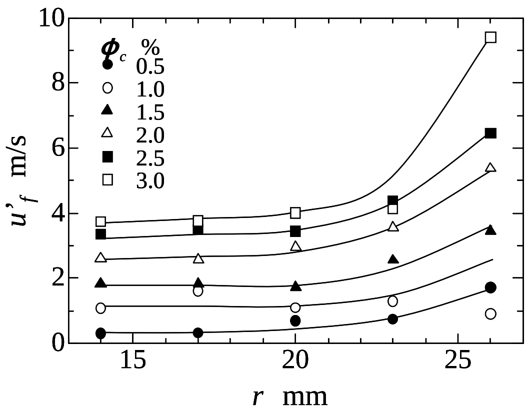

Fig. 9 Turbulent intensity profile on symmetric axis of flanged electrode.

electrode without flanges (normal electrode) on the symmetric axis of $\theta_s = 90^\circ$. The control valve opening ϕ_c is 2.0 %. Measured results were plotted and numerical results were represented by a solid and doted line in Fig. 10. It is obvious that the flanges mounted at electrode distort the flow field largely. This results in the reduction of the mean flow velocity in the swirling flow field. Numerical results have also supported it.

Figure 11 shows the reduction effect of mean velocity caused by mounting the flanges on the electrode. The ordinate represents the mean flow velocity of the swirling flow at the center position of electrode of r =20mm, $\theta_s = 90^\circ$. The abscissa represents the reduction of velocity Δu_f defined as $\Delta u_f = u_s - u_f$. Measured and numerical results appear for the control valve opening ranging from 0.5 % to 3.0 %. The reduction of the mean velocity plotted on a straight line. The fact indicates that the reduction of velocity by mounting the flange is proportional to the velocity of swirling flow. The results also indicate that the reduction rate is about 0.5, evaluated by the solid line.

Figure 12 shows the measured result of the ignition experiments. The ordinate represents the mean flow velocity of the swirling flow at the center position of electrode of r = 20 mm, $\theta_s = 90^\circ$. The abscissa represents the minimum primary current for ignition. The result shows that the minimum primary current decreases largely with an increase of mean flow velocity in the low velocity region. It become the minimum at about 5 m/s of mean flow velocity. Then the minimum primary current increase monotonously and gently. It is also obvious that the minimum primary current in flanged electrodes is less than that in the normal electrodes for whole swirling flow velocity region measured. The results also demonstrate that the flanged electrode is effective to the reduction of minimum primary current in the quiescent gas environment. It is not found that the noticeable increase of minimum primary current in the flow velocity at higher flow velocity region. It would be conceived that the flanges suppressed the increase of flow velocity around the electrodes.

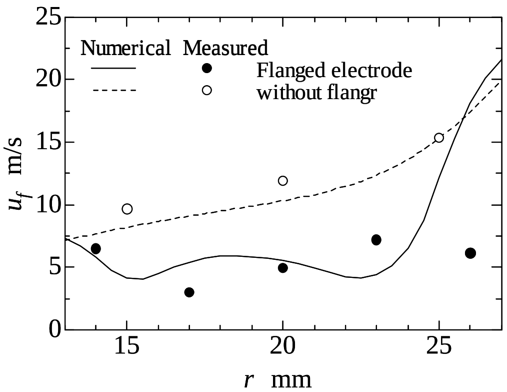

Fig. 10 Comparison of flow velocity between the flanged and normal electrode on symmetric axis.

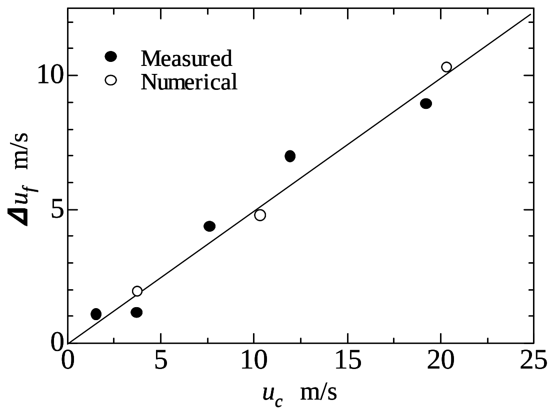

Fig. 11 Reduction effect of mean velocity caused by mounting the flanges on the electrode.

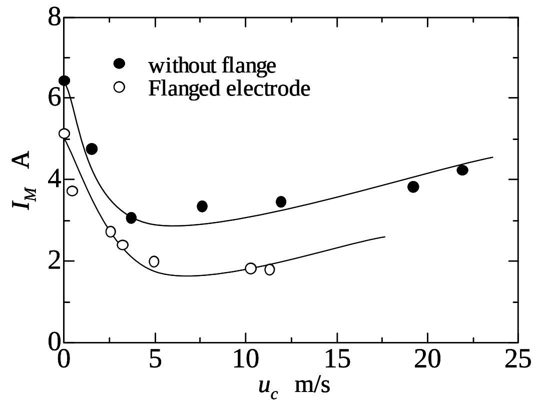

Fig. 12 Measured result of the minimum primary current.

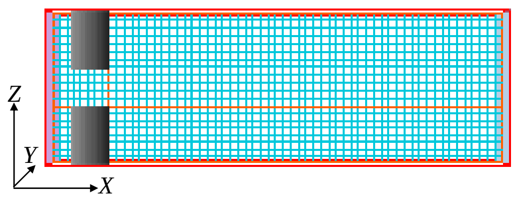

(a) Numerical domain.

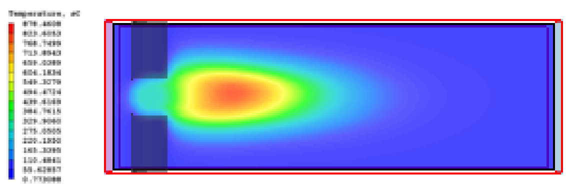

(b) An example of numerical results.

Fig. 13 Numerical analysis of supplied heat dissipation around the electrode.

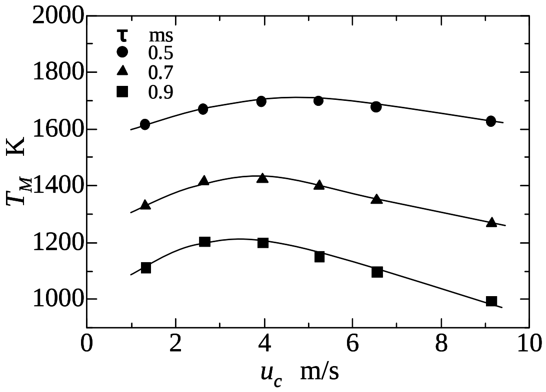

Fig. 14 Time histories of maximum temperature around the flanged electrode.

The computations for evaluating the heat dissipation supplied by spark in the flow field were carried out by almost same procedure appending the energy equation and its boundary condition. Figure 13 shows the numerical domain and an example of numerical results obtained. The grid was constituted around the electrodes along three-dimensional Cartesian coordinates, which size was 12 mm, 4 mm and 4 mm along X, Y, and Z coordinates respectively. The dimensions of the electrodes were set at the same with the experiments. The spherical heat source has been set between the electrodes as a boundary condition. The unsteady steady state of flow field and heat transportation was calculated. Flow velocity and turbulent intensity at the inlet boundary was determined by the measured results. Heat supply through the heat source is also determined from the measured results of ignition experiments. Figure 13 (b) represents an example of numerical results. This is the contour of the temperature of flow velocity of 4 m/s, and lapsed time of 0.9 ms after the start of heat supplied. It is observed that the high temperature region has been transported from the gap of the electrode by the flow.

Figure 14 shows the time histories of maximum temperature around the flanged electrode. The figure represents the extent of heat dissipation supplied at the heat source caused by flow penetration through at the gap of electrodes. The result shows that the maximum temperature in heat dissipation analysis has a peak at almost the same velocity. This suggests that the heat dissipation is one of the factors to causes the ignition energy reduction in the flanged electrodes.

4. Conclusions

Experimental study has been carried out to clarify the effect of flange mounting to the electrode for improving the ignition characteristics in lean burn environment. Primary objective of present work is to obtain the detail information about the ignition characteristics of the flanged electrode in the premixed gaseous flow field. The stable propane-air premixed swirling flow field was generated in the cylindrical constant-volume chamber for the various swirling rate, equivalent ratio. The ignition experiment was carried out using the flanged or normal electrode. The flow field was measured by using a LDV with ignition simultaneously. The effects on flow field of the flange were revealed experimentally. Three-dimensional numerical analysis has been done to support the experimental results. Effects on supplied heat dissipation of flow field around the flanged electrode have been evaluated.

Conclusions obtained in the present study are as follows:

(1) The ignition energy decreases by using the flanged electrodes for wide swirling flow velocity region.

(2) The minimum primary current decreases largely with an increase of mean flow velocity in the low velocity region.

(3) The reduction of flow velocity around the electrodes by mounting the flange are proportional to the velocity of swirling flow.

(4) The noticeable increase of minimum primary current have been observed in the flow velocity at higher flow velocity region.

(5) The maximum temperature in heat dissipation analysis has a peak at almost the same velocity. This suggests that the heat dissipation is one of the factors to causes the ignition energy reduction in the flanged electrodes.

Acknowledgements

The authors would like to thank Mr. T. Minewaki, Mr. T. Wagatsuma of Nihon University for help with the experiments and computations.

References

(1) Yamada, H., et.al., Chemical mechanistic analysis of additive effects in homogeneous charge compression ignition of dimethyl ether, Proc. Combust Inst. Vol.30(2005), pp.2773-2780.

(2) Weinrotter, M., et. Al, Laser ignition of ultra-lean methane/hydrogen/air mixtures at high temperature and pressure, Experimental Thermal and Fluid Science 29(2005), pp.569-577

(3) Zhenga, X.L., et.al., Experimental and computational study of non-premixed ignition of dimethyl ether in counterfow, Proc. Combust Inst. Vol.30(2005), pp.1104-1109.

(4)Fuse, T., et.al., Combustion characteristics of ethanol in a porous ceramic burner and ignition improved by enhancement of liquid-fuel intrusion in the pore with ultrasonic irradiation, Experimental Thermal and Fluid Science 29 (2005) , pp.467–476.

(5) Ujiie, Y., et.al., Research on the fundamental properties of flanged spark plug and application to the natural gas engine, Trans. JSME, 70-694(2004), pp. 1604-1609.